Optical and Quantum Electronics (2020) 52:21
https://doi.org/10.1007/s11082-019-2132-1

Zinc oxide: reduced graphene oxide nanocomposite film for heterogeneous photocatalysis

L. Toporovska[1] · B. Turko[1] · M. Savchak[2] · M. Seyedi[2] · I. Luzinov[2] · A. Kostruba[3] · V. Kapustianyk[1] · A. Vaskiv[4]

Received: 5 July 2019 / Accepted: 26 November 2019 / Published online: 7 December 2019

Abstract
The nanocomposite film based on zinc oxide nanostructures and reduced graphene oxide bilayer (ZnO/rGO) was synthesized, characterized and tested for the photodegradation of model organic dye (methyl orange) in water. Specifically, the nanorods of zinc oxide were obtained by the hydrothermal methods on the surface of rGO bilayers deposited on the quartz surface. The kinetics of dye photodegradation was studied via measurement of variation of the optical density at the maximum observed for the dye at 465 nm. The photodegradation efficiency of methyl orange (MO) was found to be increased from 70 to 85% when the nanocomposite material was used instead of pure ZnO nanostructures. The reaction rate constants calculated using the first-order approximation were equal to 7.2×10^{-3} min^{-1}, 1×10^{-3} min^{-1} and 1.4×10^{-2} min^{-1} for ZnO nanorods, rGO bilayer, and ZnO/rGO nanocomposite, respectively. Hence, the rate constants clearly indicate that ZnO and rGO are functioning in a synergistic manner in the fabricated nanocomposite photocatalyst. It is necessary to point that the sample keeps its integrity after multiple experiments that is important for practical applications. The obtained results evidently demonstrate potential of the nanocomposite films based on ZnO nanostructures and rGO bilayers for production of the efficient catalysts.

Keywords Nanocomposite · Heterogeneous photocatalysis · Reduced graphene oxide · ZnO nanorods

1 Introduction

Over the past decades, organic dyes have been extensively used in a number of industries, including but not limited to fabric, fiber, leather, textile, pulp and paper production, tanneries, cosmetic, pharmaceuticals and food processing (Ghowsi et al. 2014). However, it is widely recognized that the dyes are significant environment pollutants and should not be discharged to the environment with waste waters (US Enviromental Protection Agency 2005). In this respect, the cost-effective, non-toxic heterogeneous photocatalysis (HP) is

✉ L. Toporovska
liliatoporovska@gmail.com

Extended author information available on the last page of the article

widely adopted in wastewater treatment for the dye decomposition (Lam et al. 2012; Zhang et al. 2013; Kee 2017; Ahmed and Haider 2018). Among important characteristics of HP are extended use without substantial loss of photocatalytic activity, potential to reduce toxicity and complete mineralization of organics, rapid reaction rates and small footprint.

To this end, a number of properties of ZnO such as a suitable band gap (~3.37 eV), large exciton binding energy (60 meV), nontoxicity, physicochemical stability, capability to form various morphologies and low-cost production (Kulyk et al. 2011) have attracted significant attention to applications of ZnO in HP as catalytic element (Yang et al. 2002; Özgür et al. 2005; Klingshirn 2010; Kołodziejczak-Radzimska and Jesionowski 2014; Din et al. 2018). Meanwhile, combination of ZnO with graphene based materials, including (reduced) graphene oxide [(r)GO], are also receiving an increasing attention for HP applications (Xu et al. 2011; Li et al. 2012; Bai et al. 2013; An et al. 2014; Joshi et al. 2014; Qin et al. 2014, 2017; Chen et al. 2015; Rokhsat and Akhavan 2016; Kumar et al. 2017; Zhao et al. 2017; Liu et al. 2018; Xue and Zou 2018; Chauhan et al. 2019). It is shown that the enhancement of photocatalytic activity occurs owing to the hybridization of ZnO with graphene hindering the recombination of charge carries and increase the photocatalytic performance.

There are a number of publications (Li et al. 2012; Liu et al. 2012; Chen et al. 2013; Sarkar and Basak 2013) that describe the photodegradation of organic dye from water by quite effective nanopowder ZnO/(r)GO photocatalysts. However, when the powder is used it is necessary to separate a treated dye solution from the catalyst via filtration or centrifugation. It is obvious that it is more technologically effective to deposit ZnO/(r)GO catalyst on a support as a nanocomposite film. In this scenario, the catalyst/media separation is straightforward and practically effortless. However, to the best of our knowledge, there are a limited number of publications (Rokhsat and Akhavan 2016; Chauhan et al. 2019), where ZnO/(r)GO catalyst is used in form of a composite film deposited on a solid substrate. For example, Rokhsat and Akhvan fabricated the graphene oxide layer by drop-casting method on the surface of hydrothermally synthesized ZnO nanorod films. GO then was reduced to rGO using UV treatment. It was demonstrated that photocatalytic efficiency of the film is comparable with the efficiency of ZnO/rGO catalysts in powder form. The efficiency of the film was associated with high surface area provided by nanorods and the formation of heterojunction between the graphene and ZnO nanorods. Chauhan et al. fabricated nanocomposite by mixing of GO and ZnO nanoseed solution followed by spin-coating of the mixture over the Si substrate. Then, ZnO nanoflower type structures were grown from the nanoseeds. The composite film was effective in decolorization of model dye under sunlight. The improved performance of the material was attributed to the prevention of recombining of electron (conduction band) and holes (valence band) during the photocatalytic reaction.

In this work we report yet another original method for fabrication of photocatalytic ZnO/rGO film firmly anchored to SiO_2 (quartz) UV–VIS transparent substrate. Specifically, we first prepared highly conductive and transparent nanoscale rGO bilayers on the quartz surface. The bilayers were obtained via dip-coating of GO sheets encapsulated in a nanometer-thick molecular brush copolymer layer and following thermal reduction at 1100 °C in nitrogen to form rGO bilayers. The details on fabrication, structure and properties of the rGO bilayers are reported in detail in our preceding publication (Savchak et al. 2017). Next, ZnO nanorods were grown on the quartz substrates coated with rGO bilayer by the hydrothermal method using procedure reported elsewhere (Kapustianyk et al. 2016; Toporovska et al. 2017). We tested photocatalytic activity of ZnO/rGO nanocomposite film in water under ultraviolet (UV) and visible (VIS) light illumination and compare it to performance of pure rGO and ZnO films. It was found that the nanocomposite films

have significantly higher photocatalytic efficiency. It is necessary to point that the sample keeps its integrity after multiple experiments that is important for practical applications. The obtained results clearly demonstrate potential of the nanocomposite films based on ZnO nanostructures and rGO bilayers for production of the efficient photocatalysts.

2 Materials and methods

2.1 Catalyst preparation and its characterization

The surface morphology of the samples was examined using REMMA-102-02 scanning electron microscope-analyzer (JCS SELMI, Sumy, Ukraine), Hitachi S-4800 (Japan) scanning electron microscope, SOLVER P47-PRO atomic force microscope (NT-MDT Co., Moscow, Russia), and Dimension 3100 (Veeco Digital Instruments, Inc., USA) atomic force microscope. The ex situ ellipsometry measurements were performed with a serial null ellipsometer LEF-3M (Institute of Semiconductor Physics, Novorossiysk, Russia) in polarizer–compensator–sample–analyzer (PCSA) arrangement. The light source was He–Ne laser ($\lambda = 632.8$ nm).

Fabrication and characterization of rGO bilayers on quartz substrates and model Si wafers were carried out according to procedures reported elsewhere (Savchak et al. 2017). The bilayers possessed the following characteristics: thickness of ~ 3.5 nm, sheet resistance on the level of 1.370 kΩ/sq, conductivity on the level of 2300 S/cm and optical transparency of ~ 90%. Figures 1 and 2 show the morphology of the synthesized rGO bilayers. Since density of rGO is reported (Stankovich et al. 2007) to be about 2.2 g/cm^3 we can estimate that surface concentration of rGO on the quartz surface was ~ 1×10^{-3} mg/cm^2.

As it was shown in our preceding work, ZnO nanostructures grown by the hydrothermal method are quite efficient photocatalysts (Kapustianyk et al. 2016; Toporovska et al. 2017). Therefore, we used the same method for preparation of the layer of ZnO nanostructures for our nanocomposite film.

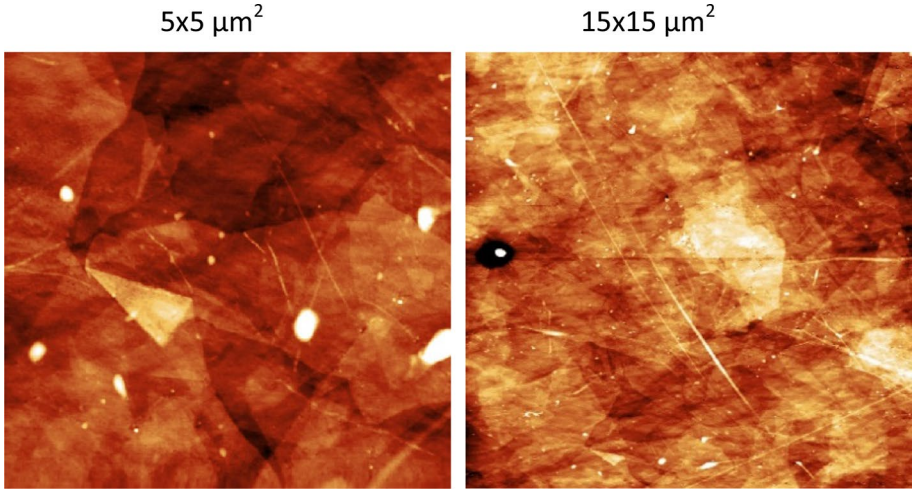

Fig. 1 AFM images of rGO-P bilayer film fabricated on quartz plate. Vertical scale: 60 and 10 nm for 15×15 μm^2 and 5×5 μm^2 images, respectively

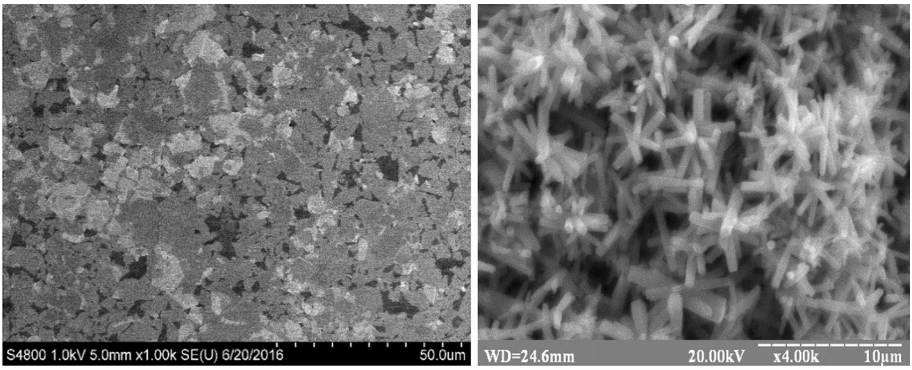

Fig. 2 Left: SEM image of rGO bilayer film deposited on SiO_2 substrate. Right: SEM image of the ZnO nanorods deposited on rGO bilayer

Figure 2 shows the typical ZnO nanostructures produced in our work by the hydrothermal method on quartz plate and quartz plate covered with the rGO bilayer. The as-prepared ZnO randomly oriented nanorods are characterized by the average length of about 4 μm and the diameter ranging from 0.4 up to 0.6 μm. We determined gravimetrically (using electronic balance WAA-210) that surface concentration of the nanorods is about 5 mg/cm^2. Since density of ZnO is known (Coltrin et al. 2008) to be 5.61 g/cm^3, the volume of ZnO nanorods on the surface can be estimated as 9×10^{-4} cm^3/cm^2. From visual observation of the ZnO layer morphology the packing density of the nanorods in the layer is between 0.4 and 0.6. Therefore, the thickness of the layer can be estimated to be between 15 and 22.5 μm.

2.2 Catalytic activity experiment

In the present study, methyl orange (MO) was chosen as model dye pollutant for ZnO mediated photocatalytic activity under UV–VIS irradiation. MO is known to cause harmful health effects for animals and humans such as eye irritation and skin irritation upon contact, respiratory tract irritation upon inhalation and digestive tract irritation upon consumption (Wei et al. 2017).

The photocatalytic activity of the samples was evaluated by measuring photocatalytic degradation of MO in water under the illumination with UV–VIS light. As it was shown in paper (Zyound et al. 2015), the largest efficiency of photodegradation is observed under the following conditions: the initial dye concentration—not more than 10 ppm and photocatalyst concentration—3 g/l. In our preceding work (Kapustianyk et al. 2016; Toporovska et al. 2017), we followed these conditions. In our current work, we placed quartz plate (active irradiated surface area of 2.2 cm^2) in a cuvette containing 3.5 mL of 5 ppm solution of MO. Therefore, concentration of active materials was: ~3.1 g/L (ZnO) and ~0.6 mg/L (rGO).

Prior to illumination, each sample (ZnO, rGO, and ZnO/rGO) was immersed in the MO solution for about 20 h in darkness in order to achieve an adsorption–desorption equilibrium state. Then, the MO solutions containing the thin film samples were irradiated cyclically every 20 min over a period of 2 h by a DRT-125 Hg-quartz lamp (with the power of

the UV–VIS source 125 Wt, among them ultraviolet was 70 Wt; with wavelengths of the irradiation 220–400 nm and light flow 1850 lm).

The desired irradiation intensity can be achieved by variation of a distance from the lamp. In this work the cuvettes containing MO solution with a sample were placed at the distance of 5 cm from a source of light. The samples were periodically withdrawn and the concentration of MO was estimated from the absorbance at 465 nm recorded with a portable fiber optic spectrometer AvaSpec-ULS2048L-USB2-UA-RS (Avantes BV, Apeldoorn, Netherlands). The detection of light in the spectrometer was carried out by a 2048 pixel CCD detector. The special software for automated computer control for this type of the spectrometer and spectra processing was used AvaSoft 8 (Apeldoorn, Netherlands).

3 Results and discussion

3.1 UV–Vis absorption property

The ex situ ellipsometry measurements of rGO bilayers on the amorphous quartz substrate were performed with employment of a single-layer model (Kostruba et al. 2015). It was found that the effective refractive index and thickness of the rGO bilayers are approximately equal to 1.8 and 13 nm, respectively. Our results of ellipsometry are well correlated with the data in this article (Shen et al. 2011).

ZnO based nanostructured materials are popularly used as cheaper catalysts for dye degradation, but the catalysis process is often found to be slow. There are two reasons: ZnO is not photoactive under visible light because of its wide band gap close to that of anatase TiO_2 (3.2–3.37 eV); the fast recombination rate of electron–hole pairs that decreases the efficiency of photocatalytic reactions (Sarkar and Basak 2013; Rommozzi et al. 2018). Therefore, in our work the bilayer of reduced graphene oxide was used in the nanocomposite for expansion of the absorption into a visible region. In order to evaluate the absorption of graphene oxide in a visible spectral range the minimum energy of electronic transition was determined. The optical absorption spectrum of rGO bilayer was measured at room temperature using the optic spectrometer. The absorption spectrum of the rGO bilayer contains two distinct maxima (Fig. 3). First of them (247 nm) corresponds to the electronic $\pi\pi^*$ transition (collective excitation) in graphite-like fragments of sp^2-hybridized carbon (Rommozzi et al. 2018). The position of this maximum, which is also called the π –plasmon or Van Hove singularity (Strouk et al. 2012), depends on the depth of oxidation of exhaust gases and varies from 225 to 240 nm for deeply oxidized exhaust gases up to 270 nm for non-oxidized graphene.

The shoulder at 290–320 nm corresponds to $n\pi$-transitions with participation of indivisible electron pairs of oxygen atoms of carbonyl groups (Rommozzi et al. 2018). In addition, the sample absorbs in the visible region. Absorption of rGO bilayer in this range is connected to the electronic transitions in sp^2-C clusters whose energy decreases with increasing of cluster size (Kupcic 2014).

In order to estimate the minimum energy of electronic transition E_{et} the analysis was carried out for the region $\lambda > 400$ nm (Fig. 3). The Tauc equation was used to determine the type of observed transition (Narayana and Jammalamadaka 2016):

$$\alpha = A(h\nu - E_{et})^n / h\nu \quad (1)$$

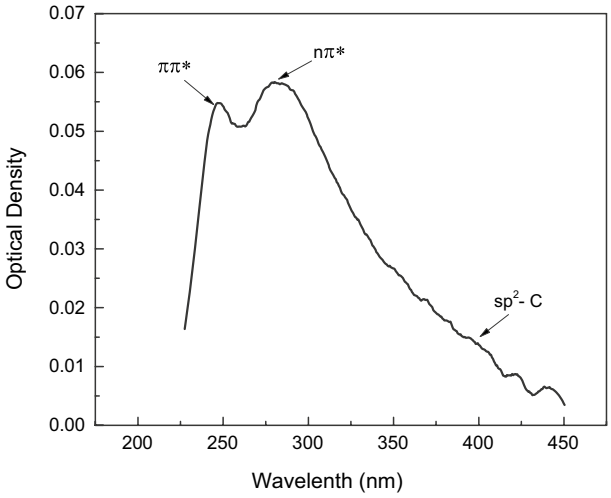

Fig. 3 The absorption spectrum of rGO bilayer

where α is the absorption coefficient, A—the constant, $h\nu$—the quantum energy of light, $n = ½$ for direct and 2 for indirect electronic transitions.

Equations (1) were presented in $\ln(\alpha h\nu)/\ln(h\nu)$ coordinates in order to determine the kind of the electron transition. The coefficient n was calculated from the slope of the obtained linear dependence. In our case the value of n was found to be 1.46. It is closer to 2, so the absorption in a visible region of spectra would be related to the indirect electronic transitions (Strouk et al. 2012). Using the Tauc equation, we determined E_{et} by extrapolation of the linear part of E vs. $(\alpha E)^{1/2}$ dependence to the abscissa axis as it is shown in Fig. 4. The obtained value $E_{et} = 2.4$ eV is consistent with the data reported elsewhere (Eda and Chhowalla 2010; Strouk et al. 2012; Zhai et al. 2015).

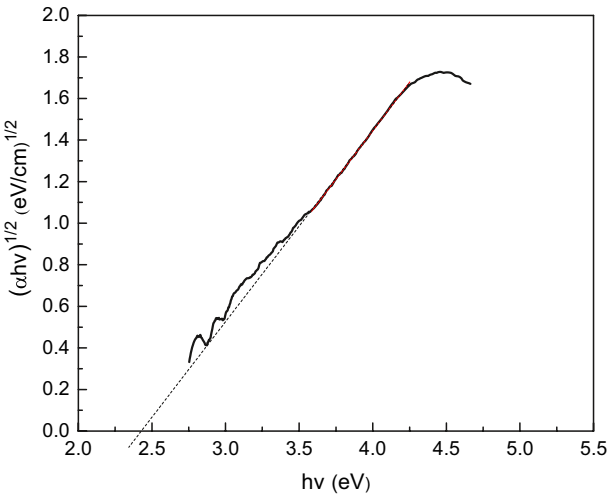

Fig. 4 Absorption spectra of rGO bilayer in $(\alpha h\nu)^{1/2} = f(h\nu)$ coordinates

3.2 Photocatalytic activity of GO, ZnO and nanocomposite ZnO/GO

Figure 5 presents the data for the photocatalytic MO degradation of three different materials deposited on the SiO_2 substrates: rGO bilayer, ZnO nanostructures, ZnO/rGO composite. It is necessary to point that irradiation of MO solution (no catalyst) at the same conditions for 120 min did not yield any measurable dye degradation. The degradation efficiency D_t was calculated by the equation (Baruah et al. 2016):

$$D_t = \left(A_0^{465} - A_t^{465}\right)/A_0^{465} \cdot 100\% \quad (2)$$

where A_0^{465} and A_t^{465}—are the dye solution optical densities at 465 nm respectively before and after irradiation for time t.

It is evident that ZnO nanorod layer has significantly higher efficiency than the layer made of rGO. In fact, after 140 min ~ 70% of MO degraded when ZnO catalyst was used. While in the presence of rGO only about 10% of the dye was decomposed during the same time period. Nevertheless, we note that the amount rGO in the cuvette is 10^4 times lower that the amount of ZnO. Therefore, it is needed to highlight that rGO is a quite effective catalyst, but it is challenging to significantly increase its surface concentration. Our data also indicate that ZnO/rGO nanocomposite film demonstrated the highest degradation efficiency, where approximately 85% of MO was photodegraded in 140 min.

We have to point that at in our experiment light cannot directly interact with rGO in the nanocomposite film. In fact, it was shown previously that, even ZnO nanorods are quite transparent at wavelength above 400 nm (Said et al. 2010), layer of ZnO nanorods significantly scatters light and at quite low thicknesses (~ 1 micron) has already very low (less than 10%) transparency in UV–VIS region (Idiawati et al. 2016; Abdulrahman et al. 2017). Therefore, ZnO layer covering rGO film and having thickness of about 15–20 micron effectively screens rGO film from light. With this in mind, the process of photodegradation catalyzed by ZnO/rGO nanocomposites can be described as follows. Under the illumination electrons are photogenerated in ZnO from the valence band to the conduction band. There is a distribution of the pair of electron–hole charges in zinc oxide, due to the strong electron interaction between rGO and ZnO. It is important to note that rGO bilayer is an acceptor of electrons, that effectively suppresses the recombination of photogenerated charge

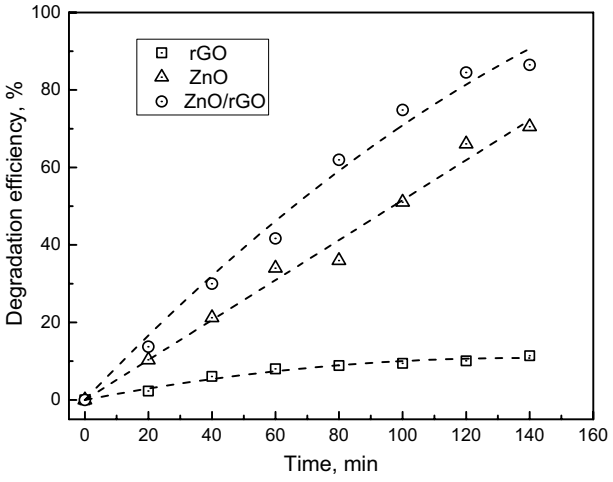

Fig. 5 Comparison of the photocatalytic performance of rGO bilayer, ZnO nanostructures and ZnO/rGO composite. Lines are guides for eye and are drawn using second order polynomial fit

carriers (Kavitha et al. 2012). The excited electrons in the conduction band are transferred to the ZnO/rGO interface, where they react with molecular oxygen and synthesize the radical superoxide radicals (O_2^-). The positively charged holes can react with hydroxide ion obtained from water, that causes formation of hydroxyl radicals ($OH^{\cdot}$) above the surface of the nanocomposite. These oxide radicals oxidize the dye to less harmful compounds. Consequently, the number of photogenerated electron–hole pairs depends on the active catalyst area and the content of rGO in the nanocomposite, which are responsible for the efficiency of the photocatalytic reaction.

The degradation of MO for ZnO nanostructures and ZnO/rGO nanocomposite is 70% and 85%, respectively (Fig. 5). For comparison, as it was reported in paper (Sarkar and Basak 2013), after 90 min of illumination, the values of MO photodegradation were found to be 70% and 85% for ZnO nanopowder and ZnO/rGO nanopowder composite, respectively. It should be noted that concentration of MO solution was 3 times larger (15 ppm) and the amount of rGO was 10 times larger than in our experiment. For comparison, for the samples in a form of layers on the substrate, reported in paper (Rokhsat and Akhavan 2016), the efficiency of photodegradation for rGO/ZnO reaches 60% in 200 min. We associate the increase in photodegradation for our nanocomposite with the fact that, in our case, we used rGO bilayer having significantly higher conductivity than rGO monolayer used in reference (Rokhsat and Akhavan 2016).

The next step in our research of photodegradation includes calculation of the reaction rate constants k using an apparent first-order model (Wang et al. 2008; Zha et al. 2015):

$$\ln\left[C_t/C_0\right] = \ln[A_t/A_0] = -kt \tag{3}$$

where t is the light irradiation time; C_0—the starting dye concentration; C_t—the dye concentration after irradiation for time t.

The representative dependences of $\ln[C_t/C_0]$ as a function of t approximated by straight lines for determination of the corresponding constant are shown in Fig. 6. The value of k for ZnO nanostructures, rGO, and ZnO/rGO nanocomposite is found to be 7.2×10^{-3} min^{-1}, 1×10^{-3} min^{-1}, and 1.4×10^{-2} min^{-1}, respectively. The correlation coefficients for the kinetic curves of reactions for ZnO nanostructures, rGO layer, and ZnO/rGO nanocomposite are $R=0.99$, $R=0.968$, and $R=0.989$, respectively. Their values reflect the adequacy of the chosen model in descriptions of the photocatalytic reaction (Savastenko et al. 2016).

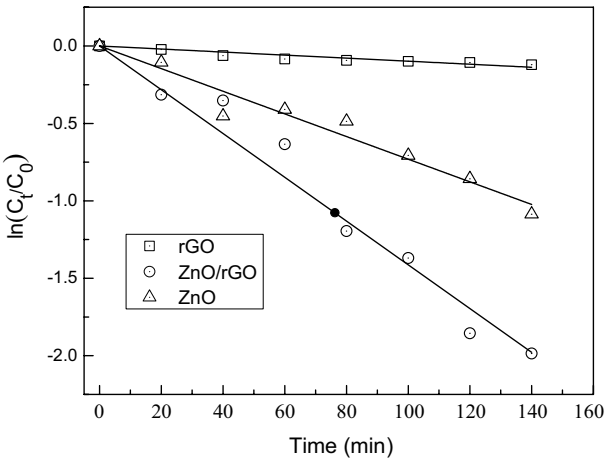

Fig. 6 The linear approximation of the kinetic curves of photocatalytic MO degradation with rGO bilayer, ZnO nanostructures and ZnO/rGO nanocomposite

We note that if ZnO and rGO in the nanocomposite are not working in coordination than the maximum possible rate constant for the nanocomposite is a summation of the constants for ZnO and rGO materials ($\sim 8.2 \times 10^{-3}$ min^{-1}) (Davis and Davis 2003). Therefore, the rate constants clearly indicate that ZnO and rGO are functioning in a synergistic manner, where the constant for the nanocomposite has significantly higher value of 1.4×10^{-2} min^{-1}.

4 Conclusion

The nanocomposite material based on zinc oxide nanorods and reduced graphene oxide bilayer was synthesized and characterized. The catalytic properties of the material in the photocatalytic degradation of MO dye was determined and compared with those for rGO bilayer and ZnO nanostructures. Our results clearly indicated that the ZnO/rGO nanocomposite film has significantly higher photocatalytic efficiency than other samples. It has been shown that the efficiency of photodegradation for ZnO/rGO nanocomposite increased by ~ 20% in comparison with the efficiency of pure ZnO nanorod layer. We suggest that the selected by us method of synthesis offers an efficient electron transfer process between ZnO and rGO layer serving as an electron collector and transporter. The reaction rate constants clearly indicate that ZnO and rGO are functioning in a synergistic manner in the fabricated nanocomposite photocatalyst. The obtained results demonstrate potential of the nanocomposite films based on ZnO nanostructures and rGO bilayers for production of the efficient catalysts.

Acknowledgements This work was supported by Ministry of Education and Science of Ukraine. Also this work was partially supported by the National Science Foundation via CMMI 1538215 and EPSCoR OIA 1655740 awards. The authors would like to thank V. V. Tsukruk and Kesong Hu of Georgia Institute of Technology (USA) for providing GO material used in this work.

References

Abdulrahman, A.F., Ahmed, S.M., Almessiere, M.A.: Effect of the growth time on the optical proprties of ZnO nanorods grown by low temperature method. Dig. J. Nanomater. Biostruct. **12**(4), 1001–1009 (2017)

Ahmed, S.N., Haide, W.: Heterogeneneous photocatalysis and its potential application in water and wastewater treatment: a review. Nanotechnology **29**, 342001–342031 (2018)

An, S., Joshi, B.N., Lee, M.W., Kim, N.Y., Yoon, S.S.: Electrospun graphene-ZnO nanofiber mats for photocatalysis applications. Appl. Surf. Sci. **294**, 24–28 (2014)

Bai, X., Wang, L., Zong, R., Lv, Y., Sun, Y., Zhu, Y.: Performance enhancement of ZnO photocatalyst via synergic effect of surface oxygen defect and graphene hybridization. Langmuir **29**(9), 3097–3105 (2013)

Baruah, S., Khan, M.N., Dutta, J.: Perspectives and application of nanotechnology in water treatment. Environ. Chem. Lett. **14**(1), 1–14 (2016)

Chauhan, P.S., Kant, R., Rai, A., Gupta, A., Bhattacharya, S.: Facile synthesis of ZnO/GO nanoflowers over Si substrate for improved photocatalytic decolorization of MB dye and industrial wastewater under solar irradiation. Mater. Sci. Semicond. Process. **89**, 6–17 (2019)

Chen, Y.L., Zhang, ChE, Deng, Ch., Fei, P., Zhong, M., Su, B.T.: Preparation of ZnO/GO composite material with highly photocatalytic performance via an improved two-step method. Chin. Chem. Lett. **24**, 518–520 (2013)

Chen, D., Wang, D., Ge, Q., Ping, G., Fan, M., Qin, L., Bai, L., Lv, Ch., Shu, K.: Graphene-wrapped ZnO nanospheres as a photocalyst for high performance photocatalysis. Thin Solid Films **574**, 1–9 (2015)

Coltrin, M.E., Hsu, J.W.P., Scrymgeour, D.A., Creighton, J.R., Simmons, N.C., Matzke, C.M.: Chemical kinetics and mass transport effects in solution-based selective-area growth of ZnO nanorods. J. Cryst. Growth **310**(3), 584–593 (2008)

Davis, M.E., Davis, R.J.: Heterogeneous catalysis. In: Davis, M.E., Davis, R.J. (eds.) Fundamentals of Chemical Reaction Engineering, pp. 133–171. McGraw-Hill, Boston (2003)

Din, M.I., Najeeb, J., Ahmad, G.: Recent advancements in the architecting schemes of zinc oxide based photocatalytic assemblies. Sep. Purif. Rev. **47**(4), 267–287 (2018)

Eda, G., Chhowalla, M.: Chemically derived graphene oxide towards large-area thin-film electronics and optoelectronics. Adv. Mater. J. **22**, 2392–2415 (2010)

Ghowsi, K., Ebrahimi, H.R., Kazemipour-Baravati, F., Bagheri, H.: Synthesize of ZnO/NPs and investigation of its effect in reduction of electrochemical charge transfer resistance; application of it for photodecomposition of calcon. Int. J. Electrochem. Sci. **9**, 1738–1746 (2014)

Idiawati, R., Mufti, N., Taufig, A., Wisodo, H., Laila, I.K.R., Fuad, A.: Effect of growth time on the characteristics of ZnO nanorods. In: 4th International Conference on Advanced Materials Science and Technology, Malang, Indonesia (2016)

Joshi, B.N., Yoon, H., Na, S.H., Choi, J.Y., Yoon, S.S.: Enhanced photocatalytic performance of graphene-ZnO nanoplatelet composite thin film prepared by electrostatic spray deposition. Ceram. Int. **40**(2), 3647–3654 (2014)

Kapustianyk, V., Turko, B., Rudyk, V., Rudyk, Y., Rudko, M., Panasiuk, M., Serkiz, R.: Effect of vacuumization on the photoluminescence and photoresponse decay of the zinc oxide nanostructures grown by different methods. Opt. Mater. **56**, 71–74 (2016)

Kavitha, Th., Gopolan, A.I., Lee, K.P., Park, S.Y.: Glucose sensing, photocatalytic and antibacterial properties of graphene-ZnO nanoparticle hybrids. Carbon **50**, 2994–3000 (2012)

Kee, W.M.: Enhanced photodegradation of dye mixtures (methyl orange and methyl green) and real textile wastewater by ZnO micro/nanoflowers. Final year Project. Sungai Long: Universiti Tunku Abdul Rahman (2017)

Klingshirn, C.: Past, present and future applications. In: Klingshirn, C., Meyer, B., Waag, A. (eds.) Zinc Oxide From Fundamental Properties Towards Novel Applications, pp. 327–328. Springer, Berlin (2010)

Kołodziejczak-Radzimska, A., Jesionowski, T.: Zinc oxide—from synthesis to application: a review. Materials **7**, 2833–2881 (2014)

Kostruba, A., Stetsyshyn, Y., Vlokh, R.: Method for determination of the parameters of transparent ultrathin films deposited on transparent substrares under conditions of low optical contrast. Appl. Opt. **54**(20), 6208–6216 (2015)

Kulyk, B., Kapustianyk, V., Krupka, O., Sahraoui, B.: Optical absorption and photoluminescence properties of ZnO/PMMA nanocomposite films. J. Phys. Conf. Ser. **289**, 012003–012009 (2011)

Kumar, V., Kim, K.H., Park, J.W., Hong, J., Kumar, S.: Graphene and its nanocomposites as a platform for environmental applications. Chem. Eng. J. **315**, 210–232 (2017)

Kupcic, I.: Damping effects in hole-doped graphene: the relaxation-time approximation. Phys. Rev. B **90**, 205426–205441 (2014)

Lam, S.M., Sin, J.C., Abdullah, A.Z., Mohamed, A.R.: Degradation of wastewaters containing organic dyes photocatalysed by zinc oxide: a review. Desalin. Water Treatm. **41**, 131–169 (2012)

Li, B., Liu, T., Wang, Y., Wang, Zh: ZnO/graphene-oxide nanocomposite with remarkably enhanced visible light-driven photocatalytic performance. J. Colloid Interface Sci. **377**, 114–121 (2012)

Liu, X., Pan, L., Zhao, Q., Lv, T., Zhu, G., Chen, T., Lu, T., Sun, Zh, Sun, Ch.: UV-assisted photocatalytic synthesis of ZnO-reduced graphene oxide composite with enhanced photocatalytic activity in reduction of Cr(VI). Chem. Eng. J. **183**, 238–243 (2012)

Liu, H.H., Xiang, M.M., Shao, X.: Graphene/ZnO nanocomposite with seamles interface renders photoluminescence quenching and photocatalytic activity enhancement. J. Mater. Sci. **53**(19), 13924–13935 (2018)

Narayana, V., Jammalamadaka, S.: Optical properties of graphene oxide under comprehensive strain using wet ball milling method. Graphene **5**, 73–80 (2016)

Özgür, Ü., Alivov, Y.I., Liu, C., Teke, A., Reshchikov, M.A., Doğan, S., Avrutin, V., Cho, S.J., Morkoçd, H.: A comprehensive review of ZnO materials and devices. J. Appl. Phys. **98**, 041301–041404 (2005)

Qin, J., Zhang, X., Xue, Y., Kittiwattanothai, N., Kongsittikul, P., Rodthongkum, N., Limpanart, S., Ma, M., Liu, R.: A facile synthesis of nanorods of ZnO/graphene oxide composites with enhanced photocatalytic activity. Appl. Surf. Sci. **321**, 226–232 (2014)

Qin, J.Q., Zhang, X.Y., Yang, C.W., Cao, M., Ma, M.Z., Liu, R.P.: ZnO microspheres-reduced graphene oxide nanocomposite for photocatalytic degradation of methylene blue dye. Appl. Surf. Sci. **392**, 196–203 (2017)

Rokhsat, E., Akhavan, O.: Improving the photocatalytic activity of graphene oxide/ZnO nanorod films by UV irradiation. Appl. Surf. Sci. **371**, 590–595 (2016)

Rommozzi, E., Zannotti, M., Giovannetti, R., D'Amato, ChA, Ferraro, S., Minicucci, M., Gunnella, R., Di Cicco, A.: Reduced graphene oxide/TiO_2 nanocomposite: from synthesis to characterization for efficient visible light photocatalytic applications. Catalysts **8**(12), 598–612 (2018)

Said, A.J., Poize, G., Martini, C., Ferry, D., Marine, W., Giorgio, S., Fages, F., Hocq, J., Boucle, J., Nelson, J., Durrant, J.R., Ackermann, J.: Hybrid bulk heterojunction solar cells based on P3HT and porphyrin-modified ZnO nanorods. Phys. Chem. C **114**(25), 11273–11278 (2010)

Sarkar, S., Basak, D.: The reduction of graphene oxide by zinc powder to produce a zinc oxide-reduced graphene oxide hybrid and its superior photocatalytic activity. Chem. Phys. Lett. **561–562**, 125–130 (2013)

Savastenko, N., Filatova, I., Chubrik, N., Gabdullin, M., Ramazanov, T., Abdullin, H., Kalkozova, V.: Enhancement of ZnO-based photocatalyst activity by RF discharge-plasma tratment. J. Appl. Spectrosc. **83**, 757–763 (2016)

Savchak, M., Borodinov, N., Burtovyy, R., Anayee, M., Hu, K., Ma, R., Grant, A., Li, H., Cutshall, D.B., Wen, Y., Koley, G., Harrell, W.R., Chumanov, G., Tsukruk, V., Luzinov, I.: Highly conductive and transparent reduced graphene oxide nanoscale films via thermal conversion of polymer-encapsulated graphene oxide sheets. ACS Appl. Mater. Interfaces **10**(4), 3975–3985 (2017)

Shen, Y., Zhou, P., Sun, Q.Q., Wan, L., Li, J., Chen, L.Y., Zhang, D.W., Wang, X.B.: Optical investigation of reduced graphene oxide by spectroscopic ellipsometry and the band-gap tuning. Appl. Phys. Lett. **99**, 141911–141913 (2011)

Stankovich, S., Dikin, D.A., Piner, R.D., Kohlhaas, K.A., Kleinhammes, A., Jia, Y., Wu, Y., Nguyen, S.T., Ruoff, R.S.: Synthesis of graphene-based nanosheets via chemical reduction of exfoliated graphite oxide. Carbon **45**(7), 1558–1565 (2007)

Strouk, A.L., Andryushin, N.S., Scherban, N.D., Ilin, V., Efanov, V.S., Yanchuk, I.B., Kuchmiil, S.Y., Pohodenk, V.D.: Photochemical reduction of graphene oxide in a colloidal solution. Theor. Exp. Chem. **48**, 1–10 (2012)

Toporovska, L.R., Hryzak, A.M., Turko, B.I., Rudyk, V.P., Tsybulskyi, V.S., Serkiz, R.Y.: Photocatalytic properties of zinc oxide nanorods grown by different methods. Opt. Quantum Electron. **49**, 408–417 (2017)

United States Environmental Protection Agency: Waste from the Production of Dyes and Pigments Listed as Hazardous 2005. https://www.epa.gov/sites/production/files/2016-01/documents/dyes-ffs.pdf (2005). Accessed 7 May 2019

Wang, C.C., Lee, C.K., Lyu, M.D., Juang, L.C.: Photocatalytic degradation of CI Basic Violet 10 using TiO_2 catalysts supported by Y zeolite: an ivestigation of the effects of operational parameters. Dyes Pigments **76**, 817–824 (2008)

Wei, R.B., Kuang, P.Y., Cheng, H., Chen, Y.B., Long, J.Y., Zhang, M.Y., Liu, Zh.Q.: Plasmon-enhanced photoelectrochemical water splitting on gold nanoparticle decorated ZnO/CdS nanotube arrays. Acs Sustainable Chem. Eng. **5**, 4249–4257 (2017)

Xu, T.G., Zhang, L.W., Cheng, H.Y., Zhu, Y.F.: Significantly enhanced photocatalytic performance of ZnO via graphene hybridization and the mechanism study. Appl. Catal. B **101**(3–4), 382–387 (2011)

Xue, B., Zou, Y.: Uniform distribution of ZnO nanoparticles on the surface of graphene and its enhancent photocatalytic performance. Appl. Surf. Sci. **440**, 1123–1129 (2018)

Yang, P., Yan, H., Mao, S., Russo, R., Johnson, J., Saykally, R., Morris, N., Pham, J., He, R., Choi, H.G.: Controled growth of ZnO nanowires and their optical properties. Funct. Mater. **12**, 323–331 (2002)

Zha, R., Nadimicherla, R., Guo, X.J.: Ultraviolet photocatalytic degradation of methyl orange by nanostructured TiO_2/ZnO heterojunctions. Mater. Chem. A **3**, 6565–6574 (2015)

Zhai, J., Yu, H., Li, H., Sun, L., Zhang, K., Yang, H.: Visible-light photocatalytic activity of graphene oxide-wraped Bi_2WO_6 hierachical microspheres. Appl. Surf. Sci. **344**, 101–106 (2015)

Zhang, D., Wu, J., Zhou, B., Hong, Y., Li, S., Wen, W.: Efficient photocatalytic activity with carbon-doped SiO_2 nanoparticles. Nanoscale **5**, 6167–6172 (2013)

Zhao, Y.T., Liu, L., Cui, T.T., Tong, G.X., Wu, W.H.: Enhanced photocatalytic properties of ZnO/reduced graphene oxide sheets (rGO) composites with controllable morphology and composition. Appl. Surf. Sci. **412**, 58–68 (2017)

Zyoud, A., Zubi, A., Helal, M.H.S., Park, D., Campet, G., Hilal, H.S.: Optimizing photo-mineralization of aqueous methyl orange by nano-ZnO catalyst under simulated natural conditions. J. Environ. Health Sci. Eng. **13**, 46–56 (2015)

Affiliations

L. Toporovska[1] · B. Turko[1] · M. Savchak[2] · M. Seyedi[2] · I. Luzinov[2] · A. Kostruba[3] · V. Kapustianyk[1] · A. Vaskiv[4]

I. Luzinov
luzinov@clemson.edu

A. Kostruba
andriykostruba@yahoo.com

V. Kapustianyk
kapustianyk@yahoo.co.uk

[1] Faculty of Physics, Ivan Franko National University of Lviv, 50, Dragomanova Str., Lviv 79005, Ukraine

[2] Department of Materials Science and Engineering, Clemson University, 515 Calhoun Dr, Clemson, SC 29634, USA

[3] Faculty of Food Technologies and Biotechnology, Stepan Gzhytskyi National University of Veterinary Medicine and Biotechnologies Lviv, 50, Pekarska Str., Lviv 79000, Ukraine

[4] Scientific-Technical and Educational Centre of Low Temperature Studies, Ivan Franko National University of Lviv, 50, Dragomanova Str., Lviv 79005, Ukraine